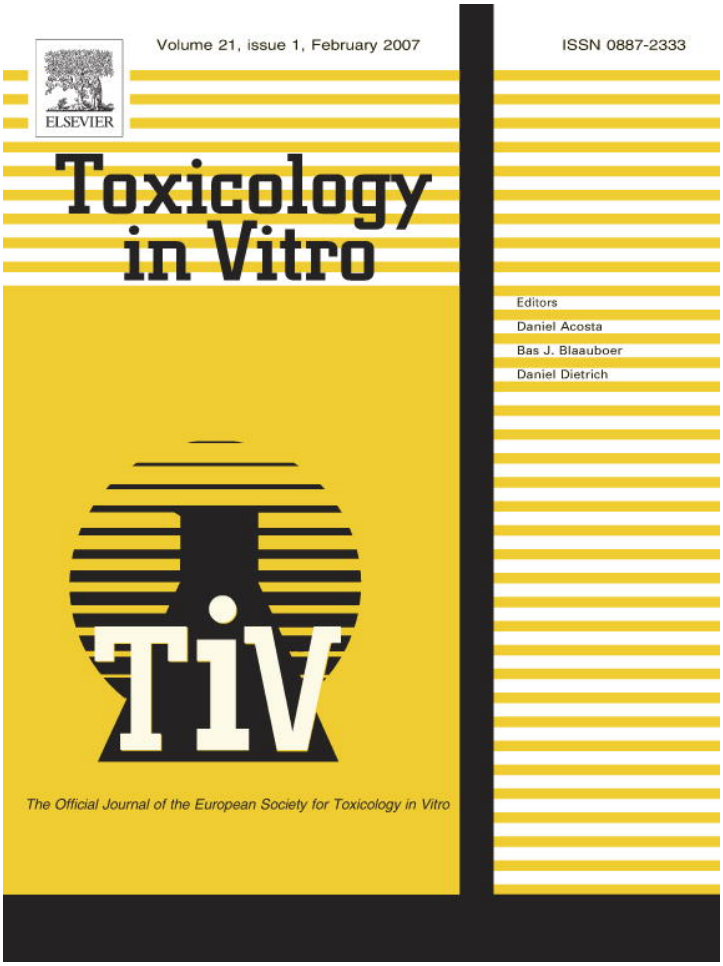

Available online at www.sciencedirect.com
ScienceDirect
Toxicology in Vitro 21 (2007) 16–24
Toxicology in Vitro
www.elsevier.com/locate/toxinvit

Aluminum toxicity triggers the nuclear translocation of HIF-1α and promotes anaerobiosis in hepatocytes

Ryan J. Mailloux, Vasu D. Appanna *

Department of Chemistry and Biochemistry, Laurentian University, Sudbury, Ont., Canada P3E 2C6

Received 12 May 2006; accepted 6 July 2006
Available online 5 August 2006

Abstract

Although aluminum (Al) is known to be toxic, the exact molecular events that enable this trivalent metal to be involved in various diseases have not been fully delineated. In this report, we show that Al promotes the translocation of the HIF-1α (hypoxia inducible factor) to the nucleus and activates the anaerobic metabolism of D-glucose. Al-exposed hepatocytes (HepG2 cells) showed a marked increase in HIF-1α that was associated with nuclear extracts. D-Glucose consumption in these Al-stressed cells was rapid as more GLUT-1 transporter was expressed. Furthermore, these Al-treated HepG2 cells were characterized with enhanced activities of such metabolic enzymes as hexokinase (HK), pyruvate kinase (PK), lactate dehydrogenase (LDH) and glucose 6-phosphate dehydrogenase (G6PDH). ^{13}C- NMR studies pointed to a metabolic profile in Al-stressed cells that favored enhanced glycolysis. HPLC analyses confirmed increased glycolytic ATP production in Al-exposed hepatocytes. These findings reveal the ability of Al to create a hypoxic environment that promotes the translocation of HIF-1α to the nucleus and stimulates the anaerobic metabolism of D-glucose.

Keywords: Al toxicity; HIF-1α; LDH; ATP; Anaerobiosis; Glucose utilization

1. Introduction

Metabolism is the foundation of all living organisms as the various metabolic networks are essential for proliferation, survival and normal biological functions (Fernie and Carrari, 2004; Middaugh and Hamel, 2005). Adaptation depends on the ability of metabolic pathways to adjust to intracellular and extracellular environmental fluxes (Feller and Gerday, 2003; Prasad Maharjan and Yu, 2005). Regulation of the glycolytic pathway is crucial for the survival of organisms facing diminished oxygen tension and/or an oxidative milieu. This metabolic route allows the production of ATP without the participation of the mitochondria (Dang and Semenza, 1999; Kim and Tchernyshyov, 2006). It has been postulated that the HIF-1α plays a pivotal role during anaerobiosis as it mediates a series of reactions that enables the cell to survive hypoxic situations (Lu and Forbes, 2002).

Under normoxic conditions, HIF-1α is hydroxylated by prolyl hydroxylase (PHD), a process that is dependent on iron (II) and α-ketoglutarate (Dery and Michaud, 2005). The hydroxylation of HIF-1α targets this transcription factor for proteosomal degradation. However, a variety of factors including reactive oxygen species (ROS), hypoxia, succinate, iron deprivation and oxidation are known to inhibit this hydroxylation process, thus favouring the stabilization of HIF-1α (Hirota and Semenza, 2006). Growth factors and pro-inflammatory cytokines are also known to aid in stabilizing and translocating this transcription factor to the nucleus (Brunelle and Bell, 2005; Selak and Armour, 2005). Co^{2+}, Ni^{2+}, and Cu^{2+} have also been shown to stabilize HIF-1α (Maxwell and Salnikow, 2004; Martin and Linden, 2005; Murphy and Sato, 2005). Activation of hypoxic and angiogenic pathways appear to be the

* Corresponding author. Tel.: +1 705 675 1151x2112; fax: +1 705 675 4844.
E-mail address: Vappanna@laurentian.ca (V.D. Appanna).

0887-2333/$ - see front matter © 2006 Elsevier Ltd. All rights reserved.
doi:10.1016/j.tiv.2006.07.013

hallmark of this transcription factor (Dery and Michaud, 2005).

Al is known to be a pro-oxidant and has recently been implicated in the generation of an oxidative milieu by aiding in the production of ROS such as $O_2^{\cdot-}$ and H_2O_2 (Exley, 2004; Singh and Beriault, 2005). Furthermore, this trivalent metal is known to interfere with iron metabolism and cells exposed to Al exhibit properties indicative of an iron-deprived environment (Middaugh and Hamel, 2005). The ability of the mitochondria to function effectively is severely restricted in the presence of Al. The involvement of this trivalent metal in various diseases such as Alzheimer's, anaemia, and dialysis encephalopathy has been suggested (Mahieu and del Carmen Contini, 2000; Zatta and Lucchini, 2003). As part of our study to decipher the molecular mechanisms that contribute to Al toxicity, we have investigated the influence of this toxic metal on various metabolic processes in human hepatocytes. Here, we demonstrate that an oxidative environment triggered by Al leads to the stabilization and translocation of HIF-1α to the nucleus. The significance of enhanced consumption of D-glucose via the glycolytic cycle and the pentose phosphate pathway is discussed.

2. Materials and methods

2.1. Cell culture

HepG2 cells (a generous gift from Dr. Templeton, University of Toronto) were seeded at 1.0×10^5 cells/ml and maintained in α-MEM containing 5% FBS and 1% antibiotics. Cells were routinely passaged and cultured in 175 cm^2 flasks and incubated with 5% CO_2 in a humidified atmosphere at 37 °C.

2.2. Al and glucose treatment

HepG2 cells were grown as described above in a 20 ml volume until they reached 70% confluency. The media was removed and the cultures were exposed to α-MEM (-FBS) containing citrate (2.5 mM citrate, control condition) or Al-citrate (2.5 mM citrate:0.5 mM $AlCl_3 \cdot 6H_2O$, Al-stressed condition) for 4 h to 24 h. The amount of Al utilized ranged from 0.2 to 13.4 μg/ml compared to 750 μg/ml found in Alzheimer's serum and the allowable limit of 0.1–10 μg/ml in drinking water (Flaten, 2001; Nayak, 2002; Smorgon and Mari, 2004). Following a 24 h exposure, control and Al-stressed cells were supplemented with 30 mM D-glucose. Cell viability was monitored by the trypan blue exclusion assay (Shannon, 1978). At the appropriate time intervals, cells were detached by trypsinization and pelleted by centrifugation at 250 g at 4 °C. Following two washings with phosphate-buffered saline (PBS), the pellet was suspended in cell storage buffer (CSB) (50 mM tris–HCl (pH 7.0), 1 mM phenylmethylsulphonylfluoride, 1 mM dithiothreitol, 250 mM sucrose, 2 mM citrate) and stored at −86 °C until further use.

2.3. Oxidized protein and lipid profiles

The Thiobarbituric Acid Reactive Species Assay (TBARS) was performed in order to evaluate the amount of oxidized lipids in the membrane, according to the method in Singh and Beriault (2005). 4×10^6 cells were isolated for this experiment. Following cell disruption, the membrane fraction was collected and solubilized in a mixture of 15% trichloroacetic acid, 0.375% trichlorobarbituric acid, and 0.25 N HCl. The reaction mixture was heated for 25 min at 95 °C. Precipitated protein was removed by centrifugation at 21000 g for 10 min. The clear supernatant was measured at 532 nm.

Determination of protein carbonyl content was performed with the dinitrophenyl hydrazine (DNPH) assay (Singh and Beriault, 2005). 1 mg of soluble protein (from 4×10^6 cells) was mixed with 1 ml of 2% (w/v) DNPH and allowed to stand for 1 h. Following precipitation of protein, the pellet was washed 3× with ethylacetate:ethanol (1:1). The resultant mixture attained after the addition of 1 ml of 6 M guanidine–HCl was read at 360 nm.

2.4. Cell fractionation

The cells were thawed and pelleted at 250 g at 4 °C for 10 min and resuspended in CSB containing 1 mg ml^{-1} of pepstatin A and 0.1 mg ml^{-1} of leupeptin. Suspended cells were mechanically disrupted using a Brunswick sonicator for 20 s in 2 s bursts. The cell homogenate was subjected to differential centrifugation to afford a cytoplasmic fraction devoid of nucleus or mitochondria (Lee and Shin, 1999; Kwik-Uribe and Reaney, 2003). Whole cells were removed by centrifugation at 100 g for 10 min at 4 °C. The pellet was discarded and the supernatant was centrifuged at 850 g to provide a nuclear pellet (Mazzola and Sirover, 2005). The nuclear pellet was resuspended in CSB and stored at −86 °C. The soluble fraction was centrifuged at 12000 g for 30 min at 4 °C to obtain a soluble fraction devoid of mitochondria. Protein concentration was determined by Bradford assay using BSA as a standard (Bradford, 1976). Proper loading and purity of cellular fractions were verified by F-actin, histone 2A, and VDAC (voltage dependent anion channel) immunoblot analysis.

2.5. In-gel activity assays

BN PAGE was performed according to a modified method of Schagger (Schagger and von Jagow, 1991; Beriault and Chenier, 2005; Singh and Chenier, 2005). Proteins were resolved using the BioRad MiniProtean™ system on a 4–16% linear gradient gel. Briefly, soluble proteins were prepared in a BN buffer (500 mM 6-amino hexanoic acid, 50 mM tris (pH 7.0)) to provide a final sample concentration of 2 mg/ml. Protein (30 μg) was loaded in each well and electrophoresed under native conditions at 80 V. Upon entering the resolving gel, the voltage was increased to 200 V. The coloured cathode buffer (50 mM Tricine,

15 mM bistris, 0.02% Coomassie G-250 (pH 7.0) at 4 °C) was replaced by a colourless cathode buffer once the running front was half way through the resolving gel. Ponceau S (0.0125% w/v) was substituted for Coomassie G-250 to allow for the visualization of PK and HK (Grandier-Vazeille and Guerin, 1996). Electrophoresis was stopped once the running front reached the bottom of the gel. The gel was then placed in equilibration buffer (25 mM tris, 5 mM $MgCl_2$ pH 7.4) for 15 min. Enzyme activity was visualized by formazan precipitation. LDH activity staining was performed using equilibration buffer, lactate (5 mM), and 0.5 mM NAD^+. The band was visualized with the aid of 0.2 mg ml^{-1} phenazine methosulfate (PMS) and 0.4 mg ml^{-1} iodonitrotetrazolium (INT) chloride. PK activity was ascertained in a similar manner using the equilibration buffer, 5 mM phosphoenolpyruvate (PEP), 0.5 mM ADP, 1 unit/ml LDH, and 0.5 mM NADH, dichloroindophenol (DCIP) (16.7 μg ml^{-1}) and INT (0.4 mg ml^{-1}) (Singh and Chenier, 2005). The activity band was excised and resolved by 2D BN-PAGE or SDS-PAGE to determine the amount of protein expressed. HK activity was also measured by monitoring the formation of glucose 6-phosphate. The reaction consisted of equilibration buffer, 15 mM glucose, 0.5 mM ATP, 2 units/ml G6PDH, and 0.5 mM $NADP^+$. The band was made apparent with PMS (0.2 mg/ml) and INT (0.4 mg/ml). A similar technique was utilized to record the enzyme G6PDH. This was achieved in an equilibration buffer containing 2 mM G6P, 0.5 mM $NADP^+$, INT (0.4 mg/ml) and PMS (0.2 mg/ml). The apparent molecular mass of each enzyme was confirmed using the appropriate standards.

2.6. Immunoblot analyses

SDS-PAGE in a discontinuous buffer system was performed according to the modified method of Laemmli (Laemmli, 1970). Samples were solubilized in 62.5 mM tris–HCl (pH 6.8), 2% SDS, and 2% β-mercaptoethanol at 100 °C for 5 min. The proteins were transferred to a Hybond ™-P polyvinylidene difluoride membrane for immunoblotting. Nonspecific binding sites were blocked by incubating the membrane in 5% non fat skimmed milk in TTBS (20 mM tris–HCl, 0.8% NaCl, 1% Tween-20 pH 7.6) for 1 h. Monoclonal and polyclonal antibodies raised against HIF-1α, GLUT-1 (Santa Cruz, CA), LDH and, GADH (Abcam, Cambridge, MA) were used to determine the expression levels of their cognate epitopes. F-actin and histone 2A (Santa Cruz, CA) were used as the loading controls. The secondary antibody consisted of horseradish peroxidase-conjugated mouse anti-rabbit, goat anti-mouse, or mouse anti-goat (Santa Cruz, CA). Detection of the desired antigen was done by incubating for 5 min at room temperature in Chemiglow (Alpha Innotech). The immunoblots were subsequently documented using the ChemiDoc XRS system (Biorad Imaging Systems). Band intensity was quantified using Alpha Innotech Software (Alpha Innotech Corporation).

2.7. D-Glucose consumption assay

Spent fluid was isolated at desired time intervals from control and Al-stressed cultures following D-glucose supplementation. Glucose uptake was monitored with a glucose assay kit (Sigma) according to the manufacturer's protocols. The assay was normalized using glucose standards.

2.8. ^{13}C- NMR studies and ATP measurement

These experiments were performed with soluble fraction isolated from control and Al exposed cells (10×10^6 cells). Soluble fractions were incubated in a microfuge tube in a phosphate reaction buffer (10 mM Na_2HPO_4, 5 mM $MgCl_2$, pH 7.4) containing 10 mM (2-^{13}C) D-glucose, 0.5 mM NAD^+, and 0.5 mM ADP. Following a 1 h incubation at 37 °C, the reaction was stopped by heating the sample for 5 min at 95 °C. The resulting mixture was subjected to ^{13}C- NMR analysis using a Varian Gemini 2000 spectrometer operating at 50.38 MHz for ^{13}C The following parameters (35° pulse, 1-s relaxation delay, 8 kilobytes of data, and 2000 scans) were routinely utilized to record the spectra. Similar experiments were performed with soluble fraction incubated with D-glucose (10 mM), NAD^+ (0.5 mM), and ADP (0.5 mM) for 15 min. Following the precipitation of the proteins by heating at 95 °C for 5 min, the reaction mixture was centrifuged for 10 min at 12,000*g*. The supernatant was collected and placed in an ice cold microfuge tube. ATP concentration was measured by an enzyme coupled assay involving HK (10 units/mL), G6PDH (10 units/mL), and $NADP^+$ (1.0 mM) (Tsang and Howell, 1988).

To further confirm the anaerobic metabolism operative in Al-stressed cells, the metabolites were analyzed by HPLC. Cytoplasm from control and Al-stressed cells was collected as described above and incubated in the presence of 10 mM glucose, 0.5 mM NAD^+, and 0.5 mM ADP in a phosphate buffer for 15 min at 37 °C. The reaction was stopped by heating the reaction mixture at 95 °C for 5 min. Protein was removed by treatment with 0.5% HPLC grade trichloroacetic acid (Sigma). The samples were then centrifuged at high speed for 2 h and filtered through a 0.22 μm filtration unit. Following dilution (1:1 ratio) with mobile phase, the metabolites were analyzed on a C_{18}-reverse phase column (Phenomenex) using an HPLC purchased from Waters. The mobile phase consisted of 20 mM K_2HPO_4 (pH 2.9 with 6 N HCl) and the column was eluted at a flow rate of 0.7 ml/min at 30 °C ambient temperature. ATP and ADP were detected at 254 nm. The retention time of the nucleotides was compared to known standards.

2.9. Analysis of Fe metabolism

The nature of the Fe–S cluster was determined spectrophotometrically by scanning 0.5 mg/ml of protein

equivalent of mitochondria from control or Al-stressed cultures. The Fe–S cluster peak attributed to 395–420 nm was monitored (Middaugh and Hamel, 2005). Aconitase, a mitochondrial enzyme, was detected by immunoblot analysis (the ACN antibody was a generous gift from Dr. R. Eisenstein, University of Wisconsin-Madison).

2.10. Statistical analysis

Data were expressed as mean ± SD. Statistical correlations of data were checked for significance using the student t test.

3. Results and discussion

To evaluate the impact of Al on the oxidative status of the hepatocytes, the HepG2 cells were treated with Al-citrate for 24 h and oxidized lipids and proteins, markers of an oxidative environment were monitored. A sharp increase in oxidized lipids and proteins were recorded in the Al-treated cells respectively (Table 1). The generation of an Al-induced oxidative stress prompted us to examine the levels of HIF-1α. HepG2 cells were exposed to citrate and Al-citrate and the soluble extracts were analyzed at various time intervals. Immunoblot assays revealed bands indicative of HIF-1α at 4 h, 8 h and 24 h. In the control

Table 1
Oxidized lipid and protein in HepG2 cells cultured in citrate or Al-citrate

	Oxidized lipids (μmol[a]/4 × 10^6 cells)		Oxidized proteins (pmol[b]/4 × 10^6 cells)	
Time (h)	4	24	4	24
Citrate	0.068 ± (0.005)	0.024 ± (0.001)	0.279 ± (0.002)	0.465 ± (0.002)
Al-citrate	0.205 ± (0.010)	0.609 ± (0.017)	0.465 ± (0.004)	1.302 ± (0.007)

$n = 3$, mean ± SD in parentheses.
[a] Malondialdehyde equivalents (μmol).
[b] Carbonyl equivalents (pmol).

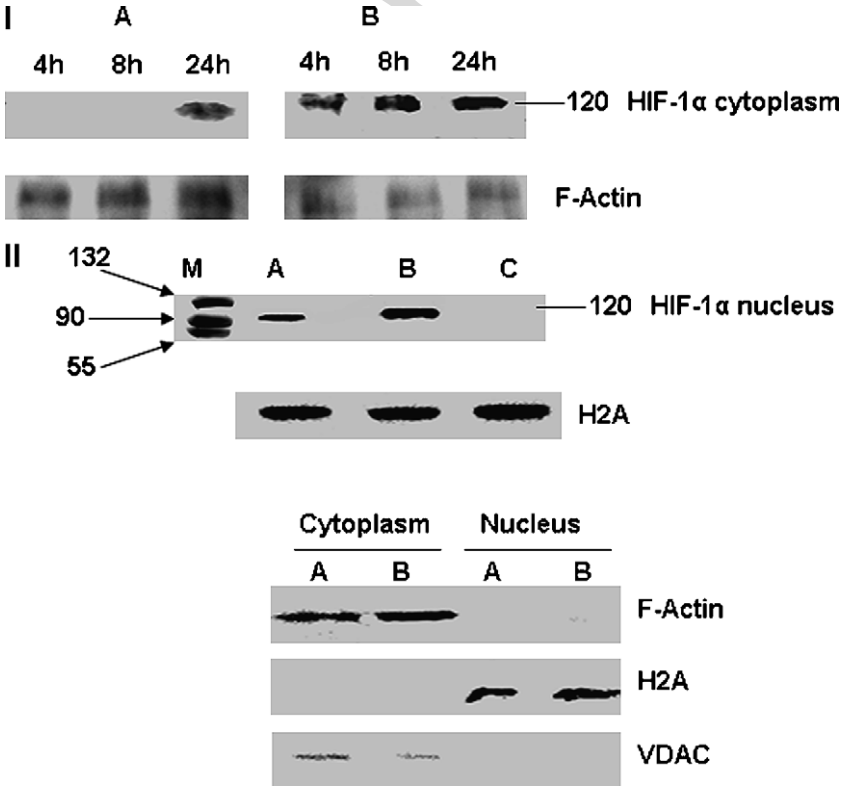

Fig. 1. Detection of HIF-1α levels in HepG2 cells isolated from (A) citrate and (B) Al-citrate cultures. (I) Immunoblot analyses of the time dependent variation of HIF-1α in HepG2 cells cultured in citrate or Al-citrate media. (II) Nuclear localization of HIF-1α measured by immunoblot. Nuclear extracts from citrate and Al-citrate cells were examined following exposure to (A) citrate, (B) Al-citrate and (C) Al-citrate stressed cells transferred into 5% FBS (note the absence of the HIF-1α respectively for 24 h). F-actin, H2A, VDAC detection were utilized as internal loading standards and to ensure cytoplasmic and nuclear extract purity.

fractions, a faint band was observed only in cells harvested at 24 h of incubation in citrate (Fig. 1, I). The nuclear fractions obtained from the Al-treated HepG2 cells did contain high amounts of HIF-1α in comparison to the nuclear fraction from the control cultures (Fig. 1, II). However, when Al-stressed cells were exposed to 5% FBS for 24 h no HIF-1α in the nucleus was observed. The absence of HIF-1α clearly points to an important role of Al in triggering this nuclear localization. Thus, the presence of HIF-1α in the nuclear and soluble extracts from the HepG2 cells points to a hypoxic response evoked by Al toxicity. To promote such an anaerobic metabolism the glycolytic cycle would be a most likely metabolic module to be affected.

^{13}C- NMR studies were performed on the soluble fractions obtained from control and Al-challenged cells. (2-^{13}C) D-glucose was utilized as the substrate in the presence of NAD^+, ADP and P_i. It was clear that a disparate metabolism was operative in these two situations. In the Al-treated cells, stronger product peaks were evident, while in control cells, a peak at 73 ppm attributable to the unreacted glucose was still significant (Fig. 2). The ATP level in the soluble fractions from the Al-exposed HepG2 cells was 2-fold higher than that observed in the control cultures (data not shown), thus pointing to an increased anaerobic metabolism in the former cells. HPLC studies did confirm the enhanced glycolytic activity and ATP production in the Al-exposed cells (Fig. 2, inset).

To further confirm the activation of glycolysis during Al stress in hepatocytes, we examined a variety of enzymes including the glucose transporter GLUT-1. Fig. 3 (I) depicts the rapid uptake of glucose in the Al-treated cells. At 1 h of incubation, approximately 55% of the D-glucose in the medium was taken up. The Al-exposed cells were characterized with GLUT-1 while the control cells did not appear to have a significant band corresponding to GLUT-1 after 1 h of incubation (Fig. 3, II). HK, an enzyme that plays a critical role in glucose metabolism was also higher in the cells cultured in Al-citrate (Fig. 4, I). To further confirm the enhanced glucose consumption as a consequence of Al toxicity, we evaluated the activity of the enzyme G6PDH, a key component of the pentose phosphate pathway and a producer of NADPH, a potent anti-oxidant. A noticeable increase in the activity of this

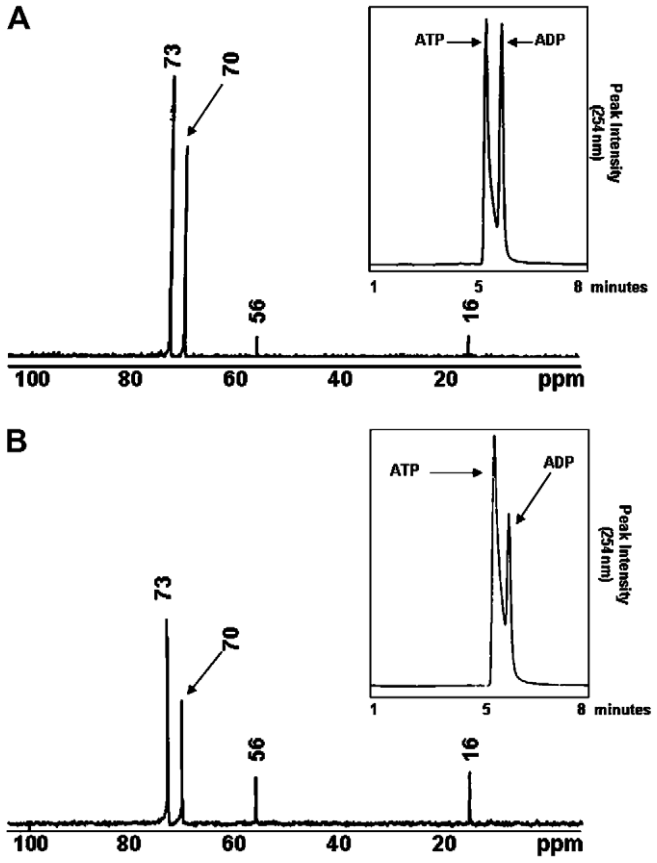

Fig. 2. Proton decoupled ^{13}C- NMR spectra of (A) citrate and (B) Al-citrate cultures. HepG2 cells were exposed to citrate and Al-citrate for 24 h and the cytoplasmic fraction was incubated for 1 h at 37 °C in a phosphate reaction buffer containing 10 mM [2-^{13}C] D-glucose, 0.5 mM NAD+, and 0.5 mM ATP. Insets: chromatographs showing the anaerobic production of ATP. Cytoplasmic fractions from control and Al-stressed cells were incubated in the presence of 10 mM glucose, 0.5 mM NAD+, and 0.5 mM ADP for 1 h at 37 °C. The fractions were then treated accordingly for HPLC analysis. ATP and ADP were referenced to standards.

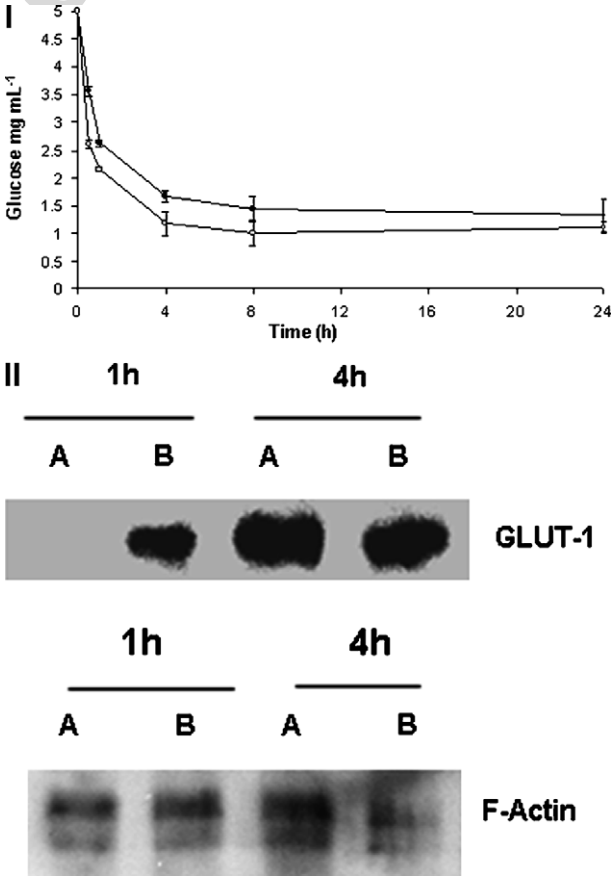

Fig. 3. (I) D-Glucose consumption in HepG2 cultures. Spent fluid was analyzed enzymatically using HK and G6PDH (Sigma). (●): citrate. (○): Al-citrate ($n = 3$, $p \leqslant 0.05$, mean ± S.D.). (II) Immunoblot analysis of GLUT-1. HepG2 cells were exposed to (A) citrate and (B) Al-citrate for 24 h and subsequently incubated with D-glucose.

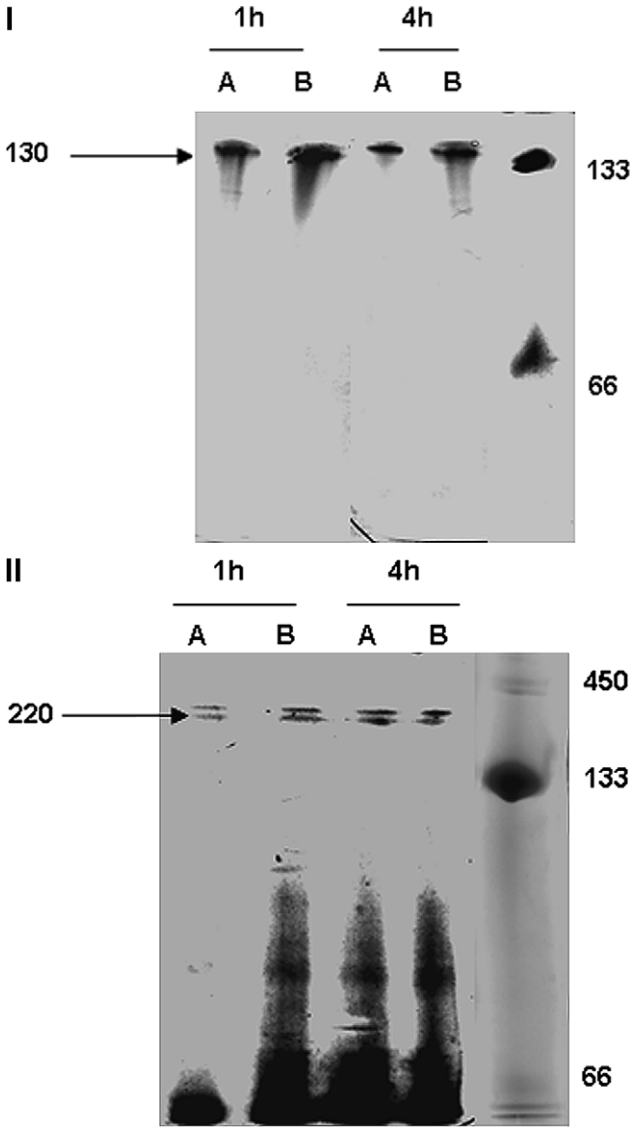

Fig. 4. Expression and activity of D-glucose utilizing enzymes in HepG2 cells exposed to (A) citrate and (B) Al-citrate. Cells were isolated at the desired time intervals following supplementation with D-glucose. (I) HK activity. Protein was resolved on a 4–16% linear gradient gel. (II) G6PDH activity. Protein was resolved on a 4–10% linear gradient gel.

enzyme was observed in the Al-exposed cells isolated at 1 h and 4 h of incubation (Fig. 4, II). LDH, an enzyme that activates glycolysis by regenerating NAD^+, was markedly upregulated in the cells subjected to Al toxicity. In this instance, Native PAGE and 2D BN-PAGE analyses revealed a sharp increment in both its activity and expression (Fig. 5, I). PK, an enzyme that mediates the phosphorylation of ADP to ATP and aids the glycolytic network was much more active in the Al-treated cells compared to the HepG2 cells grown in the control medium (Fig. 5, II). GADH, another key glycolytic enzyme involved in the metabolism of trioses was upregulated in Al-exposed cells (Fig. 5, III). Hence this evidence points to a metabolic switch favouring the production of ATP via substrate level phosphorylation, a process known to by-pass mitochondrial energy production during oxidative stress. Indeed, the mitochondria obtained from the Al-stressed cells had a disparate Fe-metabolism compared to the control hepatocytes. The characteristic absorption band at 395–420 nm, attributable to the Fe–S clusters was virtually absent in the stressed cells (Fig. 5, IV). Immunoblot analysis of aconitase (ACN), an Fe–S cluster enzyme, revealed a significant decrease in the mitochondria obtained from the Al-exposed cells.

Although Al is known to be toxic, the molecular mechanism responsible for this toxicity has not been completely elucidated (Nayak, 2002; Zatta et al., 2002). Al has been shown to act as a pro-oxidant, to create an iron-deprived environment, to mimic Ca^{2+} and to interact with cellular membrane (Zatta and Lucchini, 2003; Zafara et al., 2004; Middaugh and Hamel, 2005). The ability of Al to interfere with mitochondrial ATP formation has also been demonstrated (Dua and Gill, 2004). The data presented in this report clearly illustrate the hypoxic environment evoked by Al in hepatocytes. And as HIF-1α plays a critical role during hypoxia, the ability of Al to regulate the concentration and localization of this transcription factor was elucidated. Al-treated HepG2 cells did contain more HIF-1α in the cytoplasm and the nuclear region. Metal ions like Cu^{2+}, Ni^{2+}, and Co^{2+} have been shown to promote hypoxia and induce the synthesis of HIF-1α. Although the exact mechanism how these metals trigger HIF-1α stabilization is still undetermined, it has been postulated that PHD inhibition may be a possible contributing factor (Maxwell and Salnikow, 2004). The ability of these metals to generate ROS may also contribute in the stabilization of HIF-1α (Martin and Linden, 2005). Recently the possibility of a direct interaction between Cu^{2+} and PHD as a cause for the accumulation of HIF-1α, has also been suggested (Martin and Linden, 2005). In the present study, it is not unlikely that increased level of ROS and the reduced amount of bioavailable Fe as a consequence of Al toxicity may be contributing to the stabilization of the transcription factor. However, the possibility of direct inhibition of the PHD by Al may not be completely ruled out. The PHD is an enzyme that has an affinity for Fe and requires α-ketoglutarate. The ability of Al to interfere with these two essential cofactors may also have a negative impact on the normal activity of this hydroxylating enzyme, thus aiding in the stabilization, accumulation, and nuclear translocation of HIF-1α in the Al-exposed cells. We have also recently demonstrated the accumulation of succinate in Al-treated HepG2 cells (Mailloux and Appanna, 2006). This dicarboxylic acid has been shown to be a potent inhibitor of the hydroxylation of HIF-1α (Selak and Armour, 2005). The possible implication of α-ketoglutarate in ROS detoxification in Al-treated cells may also contribute to the inactivity of the hydroxylase. This α-keto acid has been shown to be an important cofactor for PHD (Dery and Michaud, 2005). This situation would indeed help stabilize HIF-1α and promote its migration to the nucleus.

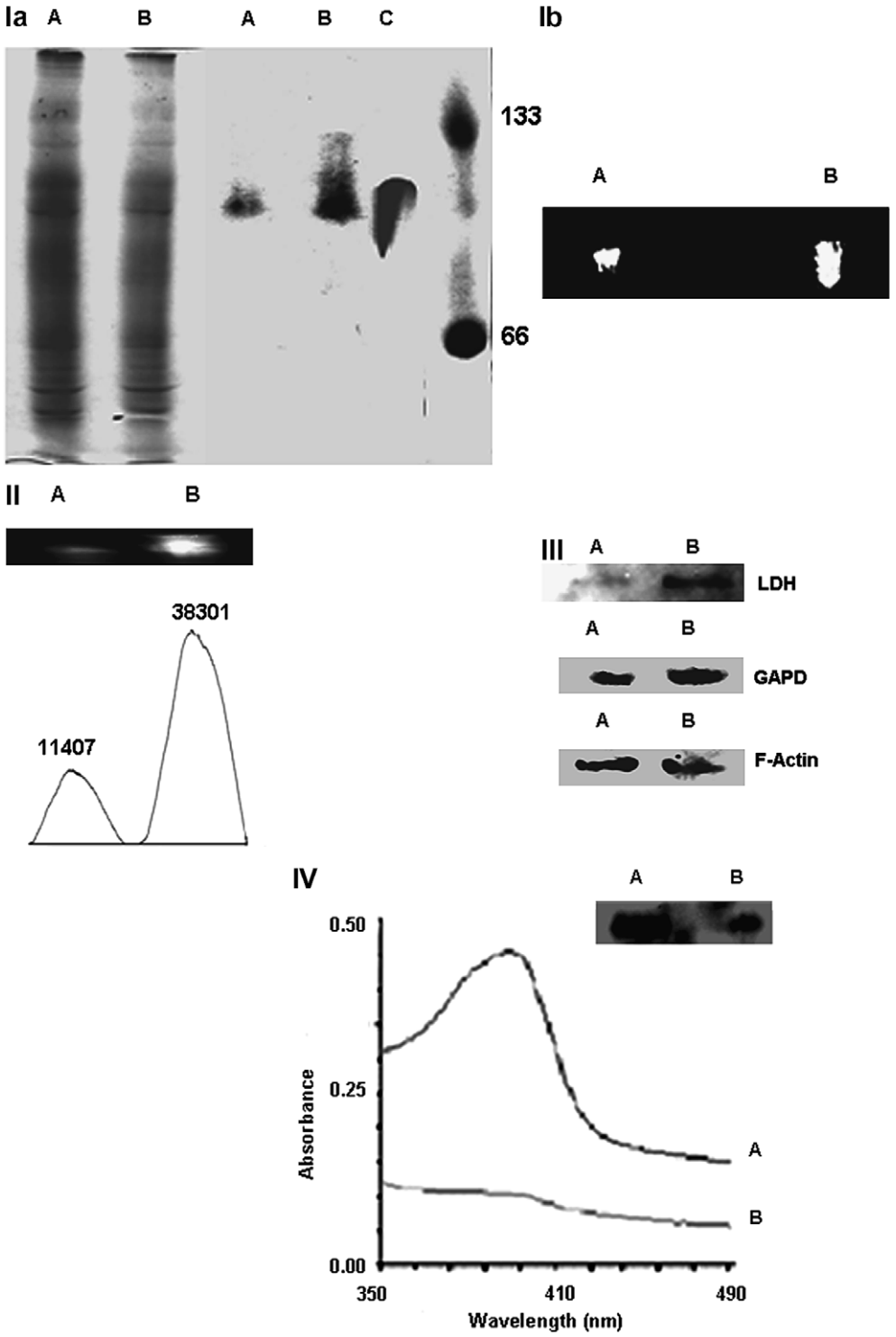

Fig. 5. In-gel activity and expression of glycolytic enzymes in the soluble fractions obtained from (A) citrate and (B) Al-citrate conditions (C) LDH standard (Sigma) Ia: Activity profile of LDH by BN PAGE. Ib: Protein expression was discerned by 2D BN PAGE of the activity band followed by silver staining. II: Activity profile of PK by BN PAGE. Bands were quantified using Scion Imaging software. III: Immunoblot detection of LDH and GAPD in cytoplasmic fraction. F-actin was utilized as a loading control. IV: Defective Fe-metabolism in Al-stressed hepatocytes: UV–Visible scan of mitochondrial extract from (A) control and (B) Al-stressed cells. Inset: The expression of ACN in mitochondrial extract from (A) control and (B) Al-stressed cells.

The accumulation of HIF-1α evoked by Al in hepatocytes enabled these cells to generate ATP via enhanced glycolysis as numerous enzymes involved in this metabolic pathway were upregulated. ^{13}C- NMR studies revealed a faster consumption of D-glucose in the cytoplasmic extract from the Al-stressed cells. The former also generated more ATP. Hence, Al appeared to be promoting glycolytic ATP production. D-glucose was rapidly consumed as its uptake

in the cell was facilitated due to the increased expression of GLUT-1 and enhanced activity of HK. Owing to the ability of the latter to generate glucose 6-phosphate, the decomposition of this metabolite via the pentose-phosphate pathway and the glycolytic cycle was further facilitated. NADPH generated by G6PDH is a key participant in the diminution of intracellular oxidative tension (Singh and Beriault, 2005). This enzyme has been shown to be upregulated during lipogenesis, oxidative stress and DNA repair (Ayene and Stamato, 2002; Berger and Ramirez-Hernandez, 2004). It is quite likely that NADPH may be promoting the reduction of the oxidative environment triggered by Al toxicity. PK and LDH, two enzymes that are pivotal in the production of ATP during anaerobiosis, had markedly increased activities in the Al-treated HepG2 cells. LDH enables the recycling of NAD^+ that subsequently further activates glycolysis (Dang and Semenza, 1999). Al clearly perturbs Fe metabolism and creates a hypoxic situation. To combat this diminished oxygen tension, the hepatocytes resort to glycolysis to produce ATP. Enzymes and their products (metabolites) are indeed the best participants in this intracellular conversation between metabolism and cellular activity as they are the direct effectors involved in energy production and the generation of a reductive environment, two critical ingredients essential for normal cellular functions. In this instance the oxidative stress triggered by Al leads to the stabilization and migration of HIF-1α into the nucleus. This transcription factor subsequently orchestrates the anaerobic glucose metabolism. Scheme 1 depicts a possible molecular mechanism how Al toxicity leads to hypoxia, HIF-1α stabilization and enhanced anaerobiosis.

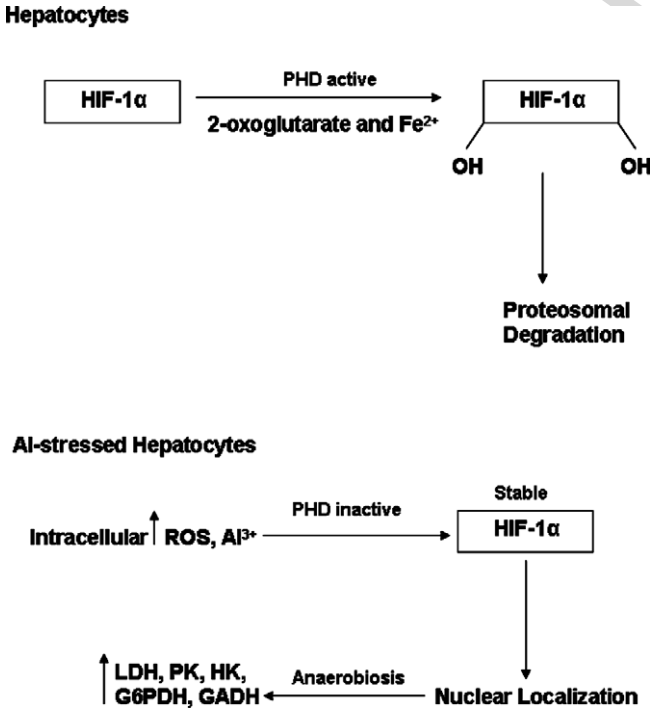

Scheme 1. A possible link between Al toxicity. HIF-1α, and stimulation of anaerobiosis.

In conclusion, our data support a direct link between Al toxicity and hypoxia in hepatocytes. The hypoxic situation leads to HIF-1α stabilization and translocation to the nucleus with the subsequent activation of D-glucose metabolism via glycolysis and pentose phosphate pathway. The latter helps in creating a reductive environment while the former generates ATP via substrate level phosphorylation. The perturbation of mitochondrial ATP production appears to be an important target of Al toxicity. Hence, Al can severely affect the energy output and thus can lead to a variety of cellular abnormalities.

Acknowledgements

This work was funded by Industry Canada and Human Resources Canada.

References

Ayene, I.S., Stamato, T.D., et al., 2002. Mutation in the glucose-6-phosphate dehydrogenase gene leads to inactivation of Ku DNA end binding during oxidative stress. J. Biol. Chem. 277 (12), 9929–9935.

Berger, F., Ramirez-Hernandez, M.H., et al., 2004. The new life of a centenarian: signalling functions of NAD(P). Trends Biochem. Sci. 29 (3), 111–118.

Beriault, R., Chenier, D., et al., 2005. Detection and purification of glucose 6-phosphate dehydrogenase, malic enzyme, and NADP-dependent isocitrate dehydrogenase by blue native polyacrylamide gel electrophoresis. Electrophoresis 26 (15), 2892–2897.

Bradford, M.M., 1976. A rapid and sensitive method for the quantitation of microgram quantities of protein utilizing the principle of protein-dye binding. Anal. Biochem. 72, 248–254.

Brunelle, J.K., Bell, E.L., et al., 2005. Oxygen sensing requires mitochondrial ROS but not oxidative phosphorylation. Cell Metab. 1 (6), 409–414.

Dang, C.V., Semenza, G.L., 1999. Oncogenic alterations of metabolism. Trends Biochem. Sci. 24 (2), 68–72.

Dery, M.A., Michaud, M.D., et al., 2005. Hypoxia-inducible factor 1: regulation by hypoxic and non-hypoxic activators. Int. J. Biochem. Cell. Biol. 37 (3), 535–540.

Dua, R., Gill, K.D., 2004. Effect of aluminium phosphide exposure on kinetic properties of cytochrome oxidase and mitochondrial energy metabolism in rat brain. Biochim. Biophys. Acta 1674 (1), 4–11.

Exley, C., 2004. The pro-oxidant activity of aluminum. Free Rad. Biol. Med. 36 (3), 380–387.

Feller, G., Gerday, C., 2003. Psychrophilic enzymes: hot topics in cold adaptation. Nat. Rev. Microbiol. 1 (3), 200–208.

Fernie, A.R., Carrari, F., et al., 2004. Respiratory metabolism: glycolysis, the TCA cycle and mitochondrial electron transport. Curr. Opin. Plant Biol. 7 (3), 254–261.

Flaten, T.P., 2001. Aluminium as a risk factor in Alzheimer's disease, with emphasis on drinking water. Brain Res. Bull. 55 (2), 187–196.

Grandier-Vazeille, X., Guerin, M., 1996. Separation by blue native and colorless native polyacrylamide gel electrophoresis of the oxidative phosphorylation complexes of yeast mitochondria solubilized by different detergents: specific staining of the different complexes. Anal. Biochem. 242 (2), 248–254.

Hirota, K., Semenza, G.L., 2006. Regulation of angiogenesis by hypoxia-inducible factor 1. Crit. Rev. Oncol. Hemat. 59 (1), 15–26.

Kim, J.W., Tchernyshyov, I., et al., 2006. HIF-1-mediated expression of pyruvate dehydrogenase kinase: a metabolic switch required for cellular adaptation to hypoxia. Cell Metab. 3 (3), 177–185.

Kwik-Uribe, C.L., Reaney, S., et al., 2003. Alterations in cellular IRP-dependent iron regulation by in vitro manganese exposure in undifferentiated PC12 cells. Brain Res. 973 (1), 1–15.

Laemmli, U.K., 1970. Cleavage of structural proteins during the assembly of the head of bacteriophage T4. Nature 227 (5259), 680–685.

Lee, W.K., Shin, S., et al., 1999. Purification and characterization of glutamate dehydrogenase as another isoprotein binding to the membrane of rough endoplasmic reticulum. J. Cell Biochem. 76 (2), 244–253.

Lu, H., Forbes, R.A., et al., 2002. Hypoxia-inducible factor 1 activation by aerobic glycolysis implicates the Warburg effect in carcinogenesis. J. Biol. Chem. 277 (26), 23111–23115.

Mahieu, S., del Carmen Contini, M., et al., 2000. Aluminum toxicity. Hematological effects. Toxicol. Lett. 111 (3), 235–242.

Mailloux, R.J., Appanna, V.D., 2006. J. Biochem. Mol. Toxic. 20 (4), 198–208.

Martin, F., Linden, T., et al., 2005. Copper-dependent activation of hypoxia-inducible factor (HIF)-1: implications for ceruloplasmin regulation. Blood 105 (12), 4613–4619.

Maxwell, P., Salnikow, K., 2004. HIF-1: An oxygen and metal responsive transcription factor. Cancer Biol. Ther. 3 (1), 29–35.

Mazzola, J.L., Sirover, M.A., 2005. Aging of human glyceraldehyde-3-phosphate dehydrogenase is dependent on its subcellular localization. Biochim. Biophys. Acta 1722 (2), 168–174.

Middaugh, J., Hamel, R., et al., 2005. Aluminum triggers decreased aconitase activity via Fe–S cluster disruption and the overexpression of isocitrate dehydrogenase and isocitrate lyase: a metabolic network mediating cellular survival. J. Biol. Chem. 280 (5), 3159–3165.

Murphy, B.J., Sato, B.G., et al., 2005. The metal-responsive transcription factor-1 contributes to HIF-1 activation during hypoxic stress. Biochem. Biophys. Res. Commun. 337 (3), 860–867.

Nayak, P., 2002. Aluminum: impacts and disease. Environ. Res. 89 (2), 101–115.

Prasad Maharjan, R., Yu, P.L., et al., 2005. The role of isocitrate lyase and the glyoxylate cycle in *Escherichia coli* growing under glucose limitation. Res. Microbiol. 156 (2), 178–183.

Schagger, H., von Jagow, G., 1991. Blue native electrophoresis for isolation of membrane protein complexes in enzymatically active form. Anal. Biochem. 199 (2), 223–231.

Selak, M.A., Armour, S.M., et al., 2005. Succinate links TCA cycle dysfunction to oncogenesis by inhibiting HIF-alpha prolyl hydroxylase. Cancer Cell 7 (1), 77–85.

Shannon, J.E., 1978. Tissue culture viability assays – a review of the literature. Cryobiology 15 (2), 239–241.

Singh, R., Beriault, R., et al., 2005. Aluminum-tolerant Pseudomonas fluorescens: ROS toxicity and enhanced NADPH production. Extremophiles 9 (5), 367–373.

Singh, R., Chenier, D., et al., 2005. Blue native polyacrylamide gel electrophoresis and the monitoring of malate- and oxaloacetate-producing enzymes. J. Biochem. Biophys. Meth. 64 (3), 189–199.

Smorgon, C., Mari, E., et al., 2004. Trace elements and cognitive impairment: an elderly cohort study. Arch. Gerontol. Geriatr. (Suppl 9), 393–402.

Tsang, W.M., Howell, M.J., et al., 1988. A simple enzymic method for the measurement of magnesium in serum and urine on a centrifugal analyser. Ann. Clin. Biochem. 25 (Pt 2), 162–168.

Zafara, T., Teegardena, D., Ashendelb, C., 2004. Nutrition Research 24, 243–259.

Zatta, P., Lucchini, R., et al., 2003. The role of metals in neurodegenerative processes: aluminum, manganese, and zinc. Brain Res. Bull. 62 (1), 15–28.

Zatta, P., Kiss, T., Suwalsky, M., Berthon, G., 2002. Coord. Chem. Rev. 228 (2), 271–284.